

Internet Appendix for “On the Relative Pricing of Long Maturity Index Options and Collateralized Debt Obligations”

PIERRE COLLIN-DUFRESNE, ROBERT S. GOLDSTEIN, and FAN YANG*

This appendix describes our calibration procedure in detail and contains figures that supplement the analysis in the published article. Figure IA.1 presents the three-year tranche spreads predicted by the model when the catastrophic jump intensity is calibrated to fit the super-senior tranche spreads. Figure IA.2 presents the three-year tranche spreads predicted by the model without the catastrophic jumps ($\lambda_C^Q = 0$). Figure IA.3 reports the time series of the two stochastic volatility state variables (V_t and θ_t), and the relative RMSE of our model for long-dated index options. Figure IA.4 compares our time-series estimates for the instantaneous market volatility with the VIX. Figure IA.5 reports the risk-neutral crash-risk intensity (λ_C^Q) calibrated to super senior tranche spreads. Figure IA.6 reports the level of idiosyncratic risk $\left(\sqrt{\sigma_i^2 + y_i^2 \lambda_{i,1}^Q}\right)$ across the different models.

*Citation format: Collin-Dufresne, Pierre, Robert S. Goldstein, and Fan Yang, 2012, Internet Appendix for “On the Relative Pricing of Long Maturity Index Options and Collateralized Debt Obligations,” *Journal of Finance*, DOI: 10.1111/j.1540-6261.2012.01779.x Please note: Wiley-Blackwell is not responsible for the content or functionality of any supporting information supplied by the authors. Any queries (other than missing material) should be directed to the authors of the article.

A. Three-Year Tranche Spreads

The model performs equally well for the three-year tranche spreads as for the five-year spreads. The results for the three-year tranche spreads with and without catastrophic jumps calibrated to super-senior tranche spreads are reported in Figures IA.1 and IA.2 respectively. Details about the procedure for jointly calibrating three- and five-year tranche spreads can be found in the following sections.

B. Numerical Solution for The Long-Maturity Option Model

We augment the standard SVCJ option model with two additional features. First, we add a second stochastic volatility state variable to better match both short- and long-maturity option prices. Second, we introduce a catastrophic jump intensity to match the super-senior tranche (30 to 100%) of the CDX. The log market dynamics ($m_t = \log M_t$) are

$$dm_t = \left(r - \delta - \bar{\mu}_y \lambda^Q - (e^{y_C} - 1) \lambda_C^Q - \frac{1}{2} V_t - \frac{1}{2} \theta_t \right) dt + \sqrt{V_t} dw_1^Q + \sqrt{\theta_t} dw_2^Q + y dq + y_C dq_C \quad (\text{IA.1})$$

$$dV_t = \kappa_V (\bar{V} - V_t) dt + \sigma_V \sqrt{V_t} (\rho_1 dw_1^Q + \sqrt{1 - \rho_1^2} dw_3^Q) + y_V dq \quad (\text{IA.2})$$

$$d\theta_t = \kappa_\theta (\bar{\theta} - \theta_t) dt + \sigma_\theta \sqrt{\theta_t} (\rho_2 dw_2^Q + \sqrt{1 - \rho_2^2} dw_4^Q) + y_\theta dq. \quad (\text{IA.3})$$

Since the dynamics are affine, the moment generating function of the log market is

$$\phi_T(u) = \mathbf{E}_0^Q [e^{um_T}] = e^{A(T) + um_0 + B(T)V_0 + C(T)\theta_0},$$

where $A(t)$, $B(t)$, and $C(t)$ solve the ODEs

$$A'(t) = (r - \delta - \bar{\mu}_y \lambda^Q - (e^{y_C} - 1)\lambda_C^Q) u + \kappa_V \bar{V} B(t) + \kappa_\theta \bar{\theta} C(t) + \lambda^Q \mathbb{E}^Q [e^{uy+B(t)y_V+C(t)y_\theta} - 1] + \lambda_C^Q (e^{uy_C} - 1) \quad (\text{IA.4})$$

$$B'(t) = -\frac{1}{2}u + \frac{1}{2}u^2 - \kappa_V B(t) + \frac{1}{2}\sigma_V^2 B(t)^2 + \rho_1 \sigma_V u B(t) \quad (\text{IA.5})$$

$$C'(t) = -\frac{1}{2}u + \frac{1}{2}u^2 - \kappa_\theta C(t) + \frac{1}{2}\sigma_\theta^2 C(t)^2 + \rho_2 \sigma_\theta u C(t), \quad (\text{IA.6})$$

where

$$\mathbb{E}^Q [e^{uy+B(t)y_V+C(t)y_\theta} - 1] = \frac{e^{u\mu_y + \frac{1}{2}u^2\sigma_y^2}}{(1 - \mu_V B(t))(1 - \mu_\theta C(t))} - 1. \quad (\text{IA.7})$$

The boundary conditions are

$$A(0) = B(0) = C(0) = 0. \quad (\text{IA.8})$$

We apply the Fast Fourier Transform (FFT) to the characteristic function $\phi_T(iv)$ to get the risk-neutral market distribution at horizon T , and use the distribution to price European options. Details about the FFT application on option pricing can be found in Carr and Madan (1999).

C. Calibration Procedure for the Market Model

Details on the calibration of market dynamics are described below. We bootstrap the daily zero-coupon curve from swap rates of one, two, three, four, five, and six-year maturities using the extended Nelson-Siegel (1987) approach. Market dividend yields are from OptionMetrics. Other parameters are chosen to fit five-year option implied volatilities with moneyness from 0.5 to 1.5 with 0.1 increments and one-year at-the-money options. Option prices are computed using FFT. When fitting these options, we

set $\rho_1 = -0.48$ following BCJ,¹ and optimize other parameters (Θ) of the option model to minimize the overall relative root mean square errors (RMSE) of implied volatilities for every series:

$$\Theta^* = \arg \min_{\Theta} \left\{ \sum_t RMSE_t(\Theta; V_t^*, \theta_t^*)^2 \right\}. \quad (\text{IA.9})$$

Here, the overall relative RMSE is computed as the sum of the minimized relative RMSE of the implied volatilities (σ_n) of one-year at-the-money options and five-year options with 11 different moneyness for each date (t) over state variables (V_t and θ_t) as

$$RMSE_t(\Theta; V_t^*, \theta_t^*) = \sqrt{\min_{V_t, \theta_t} \sum_n w_n \left(\frac{\sigma_{n,model}(\Theta; V_t, \theta_t)}{\sigma_{n,data}} - 1 \right)^2}. \quad (\text{IA.10})$$

In this formula, (V_t^*, θ_t^*) are the optimized state variables and w_n is the weight on option n . We put more weight on fitting the one-year at-the-money option than five-year options to perfectly match the level of short-term market volatility.

For the model with crash-risk intensity calibrated to super-senior tranches, we adopt an iterative procedure starting from the parameters obtained without crash risk. Because of the heavy computational costs of pricing the super-senior tranche using Monte Carlo simulation, we use a relatively simple approach to calibrate λ_C^Q . We assume that the catastrophic jump intensity is piece-wise linear: a constant equal to $\lambda_{C,3}^Q$ for the first three years, and equal to $\lambda_{C,5}^Q$ thereafter. We first use the parameters obtained with $\lambda_C^Q = 0$ and simulate the model to compute super-senior tranche spreads (S_L, S_H) for two given catastrophic jump intensities ($\lambda_{C,L}^Q, \lambda_{C,H}^Q$). Then, for each super-senior spread observed in the data (S), we compute the $\lambda_{C,i}^Q$ parameters using linear interpolations. Specifically, we find $\lambda_{C,3}^Q$ to match the three-year super-senior tranche spread first and then $\lambda_{C,5}^Q$ to match the five-year super senior tranche spread (given $\lambda_{C,3}^Q$). Finally, we

¹BCJ advocate using some time-series information when theory restricts risk-neutral and physical measure parameters to be the same and the latter are fairly well estimated from data. We found this parameter to be difficult to pin down from the cross-section alone, and therefore use BCJ's estimate.

recalibrate option parameters and iterate if necessary. We find that the super-senior tranche spreads are fairly insensitive to changes in the remaining parameters and state variables. Therefore, this approach works fairly well with a single set of $\lambda_{C,L}^Q$ and $\lambda_{C,H}^Q$ even in time-series calibrations. In fact, we find that during the pre-crisis period, we do not even need to iterate the calibration procedure to achieve a good fit. Therefore, we report only one set of parameters for the non-crash parameters. During the crisis period, however, we report two sets of parameters as the interaction between crash parameters and other parameters is more significant. In Figure IA.3 below we present the time series of $RMSE_t$ as well as the implied volatility state variable dynamics for V_t and θ_t . Further, as a check that our calibration is sensible, we report in Figure IA.4 the fitted instantaneous volatility ($\sqrt{V_t + \theta_t}$) and compare it with the VIX index. While theoretically these two processes are different, we can expect to find a high correlation between them and it is therefore comforting to see that they track each other fairly closely. Lastly, in Figure IA.5, we report the time series of crash intensities. It is clear that before the crisis the crash intensity is close to zero. There is a small increase around the May 2005 period corresponding to the downgrade of Ford and GM. But mostly the intensity is insignificantly different from zero. However, mid-2007 we see a tremendous increase in the crash intensity to 100bps in 2008. We emphasize that the five-year line on the graph really corresponds to the three into five forward intensity, given the way we parameterize the intensity step function. The graph therefore also shows that the perceived forward crash intensities are quite a bit higher both during the May 2005 event and the crisis, indicating that this affects the five-year super-senior tranche more than the three-year tranche. At its maximum, the super-senior implied catastrophe occurs once every hundred years, with a magnitude that far exceeds even the Great Depression (since super-senior insurance pays off only if more than 37.5% of the investment grade portfolio defaults, given our 20% recovery assumption).

C.1. Estimation of Firm Level Statistics

Here we explain how we construct the quantities reported in Table II of the main text.

The risk-free rate and S&P 500 index dividend yield are time-series averages for each six-months period corresponding to the series. Table II reports these estimates over the series in our sample.

The leverage ratio is defined as book debt divided by the sum of book debt and market equity, where book debt is computed as by the sum of short-term debt and long-term debt from quarterly Compustat. If any of these numbers are missing, we use their corresponding items in annual data. Table II reports the leverage ratio averages over firms and time series of a five-year moving window that ends at the initial date of every series.

We estimate asset betas and idiosyncratic volatilities using return data for all firms that comprise the index. Similar to the method of estimating asset volatility in Schaefer and Strebulaev (2008), we first compute asset returns using the average of equity returns and debt returns weighted by leverage ratios and then use a CAPM regression to estimate asset betas and idiosyncratic volatilities. Because all collateral firms are investment grade, we use the returns on LQD (an exchange-traded fund of investment grade corporate bonds) to proxy for debt returns. S&P 500 index excess returns are used as the market factor. Within a five-year moving window that ends at the initial date of every series, we regress the time series of asset excess returns of each firm on the market factor to estimate asset betas. Asset idiosyncratic volatility is estimated as the

standard deviation of the regression residuals.² Averages of asset betas and idiosyncratic volatilities over firms for every series are reported in Table II.

The aggregate asset payout ratio of collateral firms is estimated by taking the average of the aggregate equity dividend yield and the corporate bond yield weighted by the average leverage ratio of each series. For the aggregate equity dividend yield we use the S&P 500 index dividend yield. The corporate bond yield is calculated by summing the risk-free rate and the average investment grade CDS spread, which is approximated by the time-series average five-year CDX index spread within the on-the-run period of each series.

C.2. Calibration of Idiosyncratic Intensity Parameters

Here we explain the method used to calibrate the idiosyncratic intensity step function to match the term structure of CDX spreads. We define the vector $X_t = \{x_{1,t}, x_{2,t}, \dots, x_{9,t}\}$ with the following components: for $i \in (1, 5)$, $x_{i,t}$ represents the idiosyncratic jump intensities λ_i^Q ; $x_{6,t}$ is the three-year catastrophic jump intensity ($\lambda_{C,3}^Q$); $x_{7,t}$ is the five-year catastrophic jump intensity ($\lambda_{C,5}^Q$); and $x_{8,t}$ and $x_{9,t}$ are the stochastic volatility variables (V_t and θ_t).

First, we set $\lambda_{C,3}^Q$, $\lambda_{C,5}^Q$, V_t , and θ_t to their time-series average values and calibrate $\bar{\lambda}_j^Q$ to the average CDX index using a linear interpolation procedure similar to the method described in Section C of the Internet Appendix. Second, we consider deviations for each state variable $x_{i,t}$ in a region ($x_{i,L}$ and $x_{i,H}$) and simulate the model to price CDX spreads ($S_{idx,j}$) with all maturities (j equals one to five years). Third, we use this information to compute a CDX spread sensitivity matrix (M) to state variables by regressing different sets of $S_{idx,j}$ (where j equals one to five years) on their corresponding state variables

²This estimate tends to underestimate asset idiosyncratic volatility. Real idiosyncratic volatility should be higher, which reduces senior tranche spreads even more. LQD is an aggregate index of investment grade bond returns. Idiosyncratic bond volatility is diversified. Therefore, when we use it to proxy for the return on the debt of the collateral firms, we underestimate the asset idiosyncratic volatility.

(X_t) . Fourth, we invert the part of M that corresponds to idiosyncratic jump intensities to back out λ_j^Q from CDX index data with other state variables calibrated as described in previous sections. To accelerate the process, we simulate only one firm to price the CDX index spreads rather than 125 firms because CDX indices only depend on the marginal distribution of defaults.

The estimated time series of idiosyncratic jump intensities are shown in Figure 3 in the main text. As can be seen when comparing to Figure 5, it is clear that the one- and two-year intensities directly capture the credit spread risk embedded in short-term CDX spreads (indeed, the approximation that the spread is equal to the risk-neutral intensity times loss given default works almost perfectly). At longer maturities this approximate relation no longer holds as well, since the possibility of default due to diffusion shocks becomes more likely. When comparing the calibration with and without catastrophic risk, one observes that the one-year intensity in the case without catastrophic risk is basically the sum of i) the idiosyncratic intensity estimated when there is catastrophic risk and ii) the catastrophic intensity, as one would expect, since in the latter case there are two sources of jump risk that can lead to early default. The presence of sizable catastrophic risk reduces the size of the idiosyncratic jump intensity required to match the large short term credit spreads. We also see from the term structure of intensities that during the pre-crisis period the intensities are fairly flat or increasing, whereas during the crisis period the intensities are flat or decreasing as a function of maturity, reflecting different slopes in the term structure of index spreads.

Figure IA.6 shows the estimated total idiosyncratic risk $\left(\sqrt{\sigma_i^2 + y_i^2 \lambda_{i,1}^Q}\right)$ across the different models. During the pre-crisis period, there is only a small difference in the estimated total idiosyncratic risk implied by our models with idiosyncratic jump risk (for both the $(\lambda_C^Q > 0, \lambda_i^Q > 0)$ and $(\lambda_C^Q = 0, \lambda_i^Q > 0)$ models) relative to the time-series estimates of idiosyncratic asset volatility ($\lambda_i^Q = 0$). This is because the calibrated idiosyncratic jump intensities are rather small in the pre-crisis period. However, since

credit spreads widen tremendously across all maturities during the crisis, and so much more than the systematic jump risk implied from the index options data, our estimates for idiosyncratic jump intensities become quite large (on the order of 200bps). This in turn leads to a much larger estimate for total idiosyncratic risk during the crisis – about 50% larger than our pre-crisis time-series estimates.

References

Nelson, C., and A. Siegel, 1987, Parsimonious modeling of yield curves, *Journal of Business* 60, 473–489.

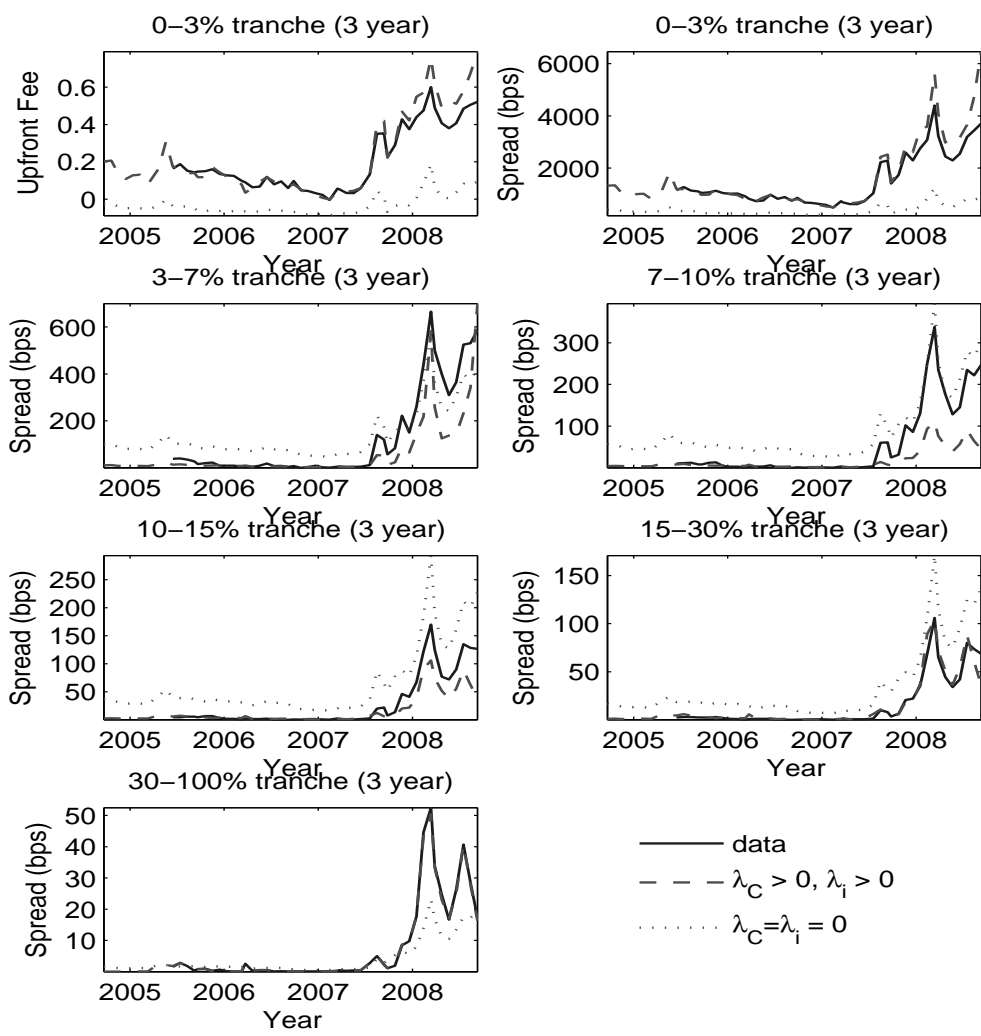


Figure IA.1. Time series of three-year tranche spreads. Predicted time series of spreads for the 0 to 3% up-front premium, 0 to 3% running premium, 3 to 7%, 7 to 10%, 10 to 15%, and 15 to 30% three-year CDX tranches for various model specifications. “data” are the historical data. $\lambda_C > 0, \lambda_i > 0$ denotes our benchmark model with idiosyncratic jumps fitted to the one- to five-year term structure of CDX, and catastrophic jump intensity fitted to the super-senior tranche. $\lambda_C = 0, \lambda_i = 0$ has neither catastrophic nor idiosyncratic jump risk.

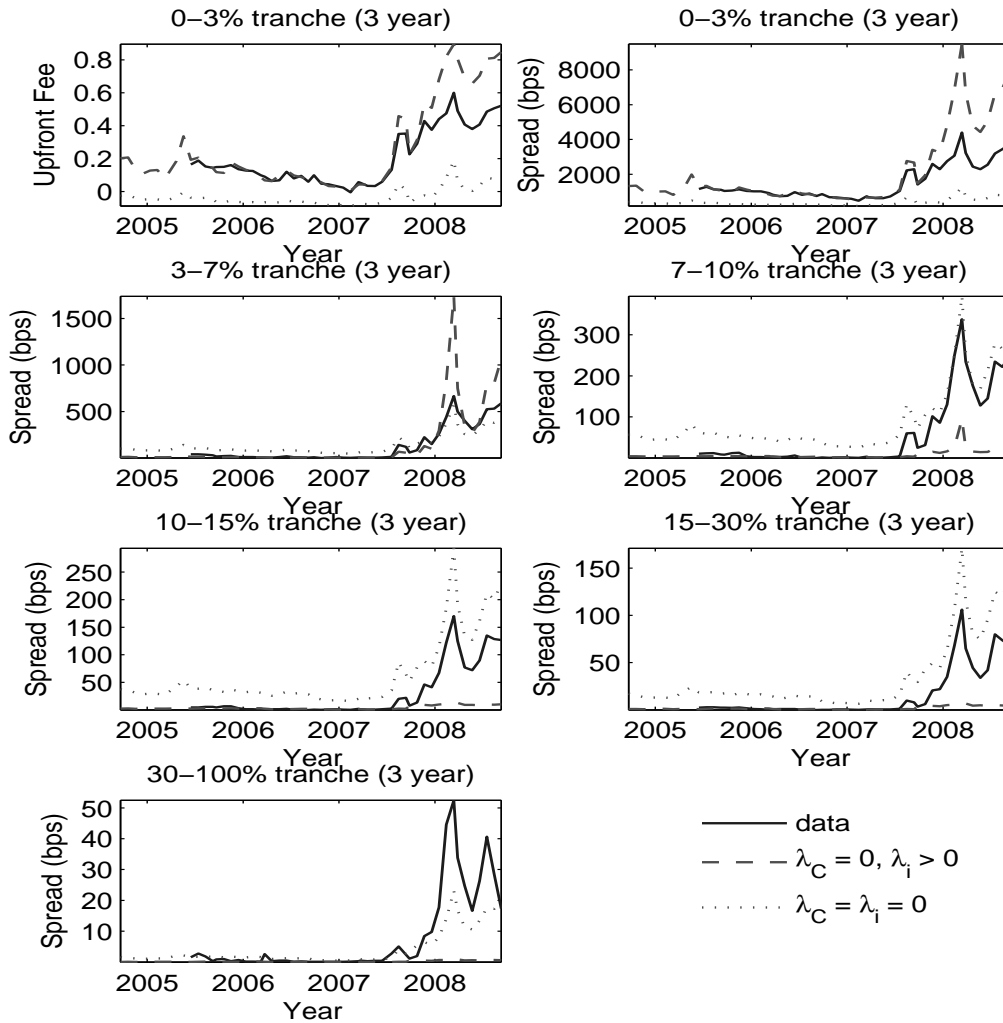


Figure IA.2. Time series of three-year tranche spreads without catastrophic risk. Predicted time series of spreads for the 0 to 3% up-front premium, 0 to 3% running premium, 3 to 7%, 7 to 10%, 10 to 15%, and 15 to 30% three-year CDX tranches for various model specifications. “data” are the historical data. $\lambda_C = 0, \lambda_i > 0$ denotes our model with idiosyncratic jumps fitted to the 1 to 5 year term structure of CDX, but where we do not allow for catastrophic jumps (i.e., systematic jumps are extracted solely from index options). $\lambda_C = 0, \lambda_i = 0$ has neither catastrophic nor idiosyncratic jump risk.

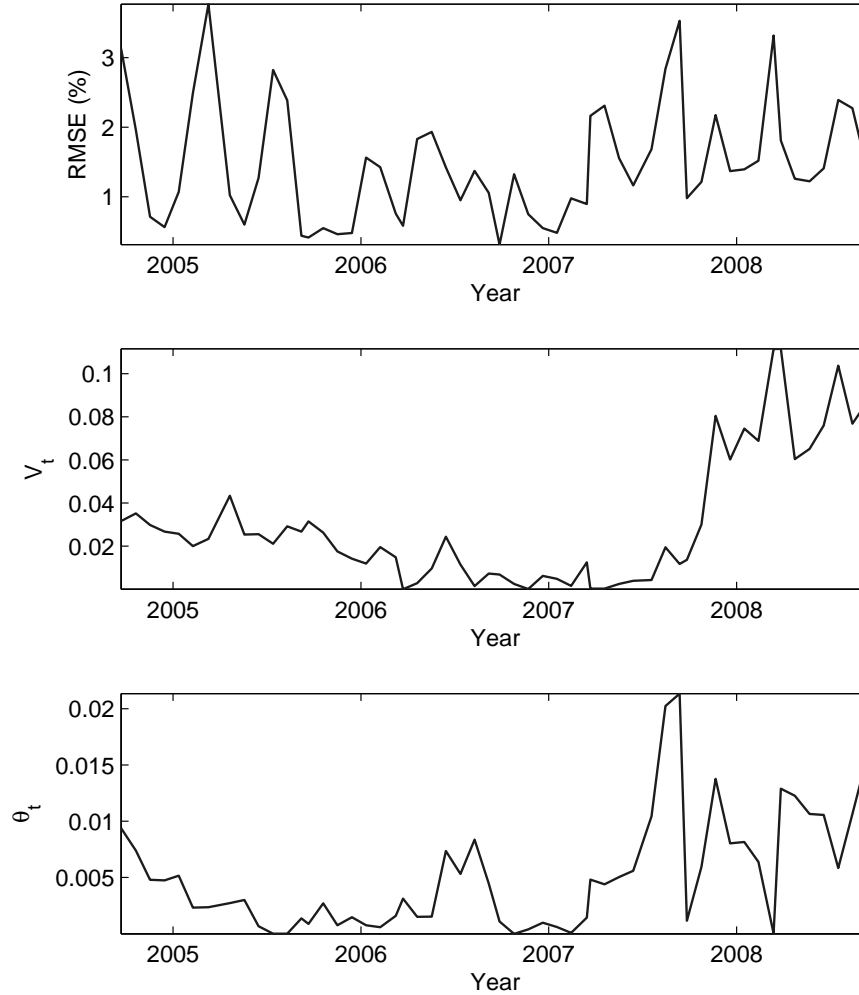


Figure IA.3. Volatility state variables. Estimated volatility state variables (V_t and θ_t defined in equations (2) and (3) of the main text) inverted from at-the-money one-year and 11 in-the-money, at-the-money, and out-of-the-money five-year option prices based on our option pricing model using the parameters presented in Table 1 of the main text. We also plot the RMSE for the panel data of options we fit every day.

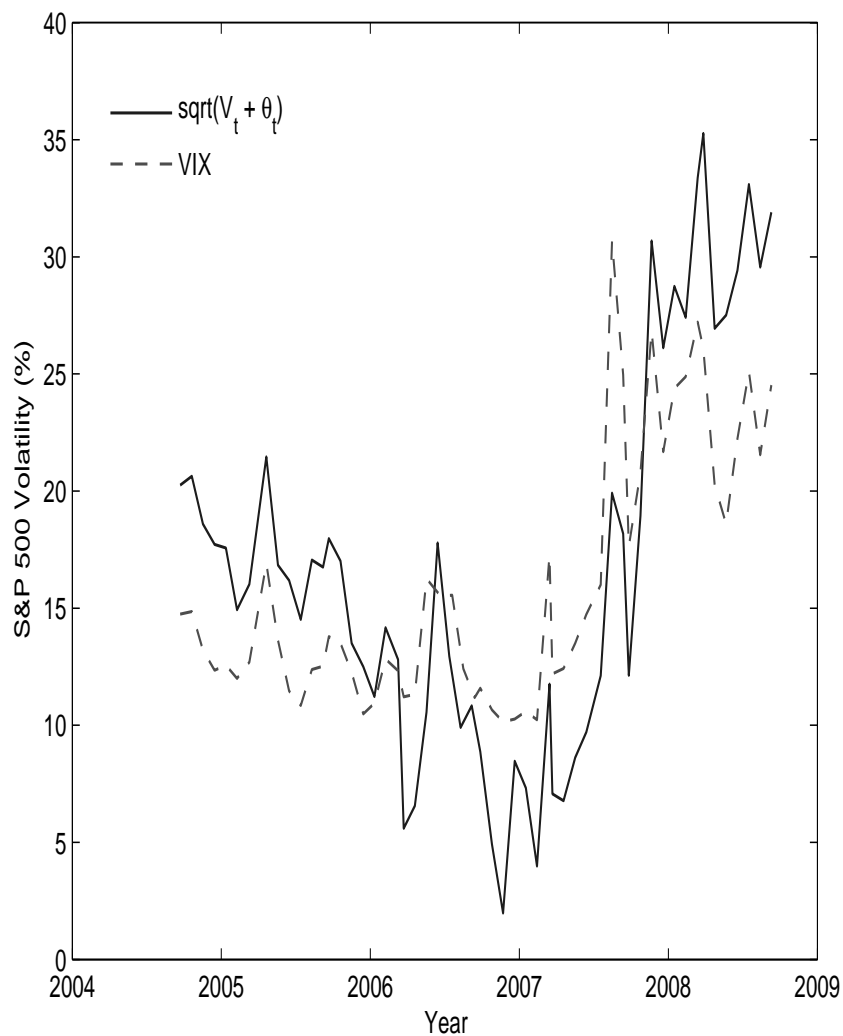


Figure IA.4. Instantaneous market return volatility. Estimated instantaneous volatility $\sqrt{V_t + \theta_t}$ of the market return, where the volatility state variables (V_t and θ_t defined in equations (2) and (3) of the main text) are inverted from at-the-money one-year and 11 in-the-money, at-the-money, and out-of-the-money five-year maturity option prices based on our option pricing model using the parameters presented in Table 1 of the main text. We also plot the VIX along side our instantaneous volatility to give a sense of the reasonableness of the fitted latent volatility state variables.

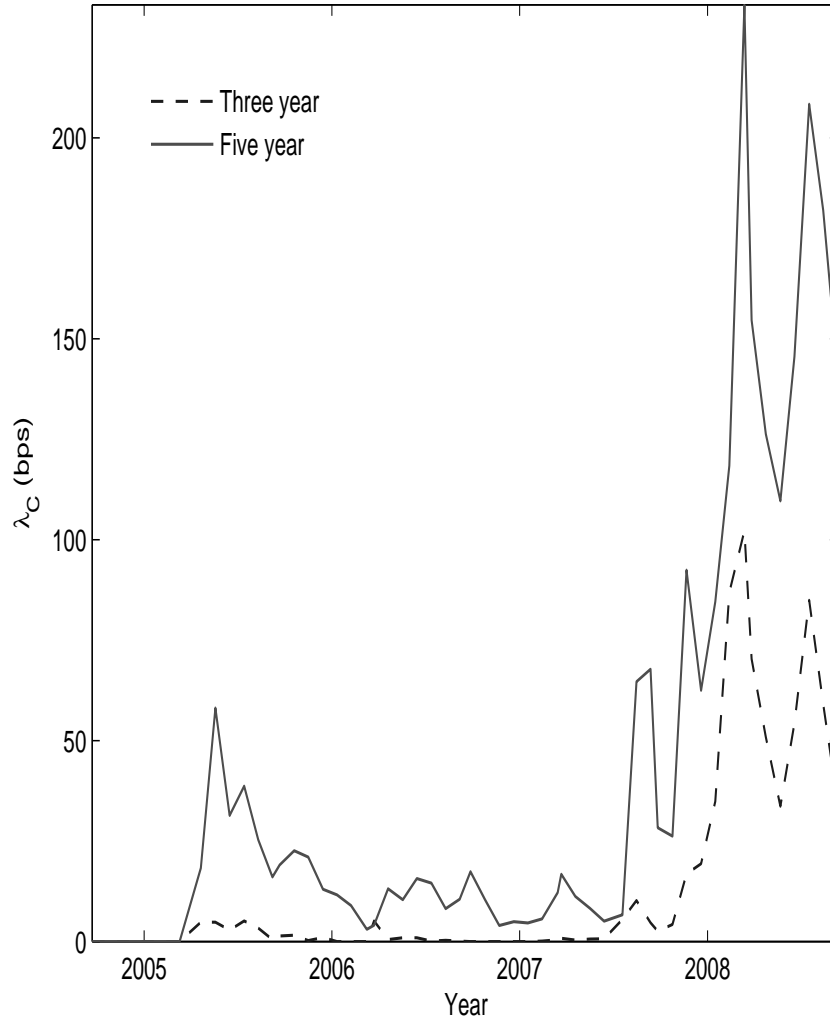


Figure IA.5. Estimated crash risk intensity. As explained in section IA.C.2 we calibrate λ_C^Q (the risk-neutral catastrophic jump intensity) to match perfectly super-senior tranches with three- and five-year maturity as well as S&P 500 index options.

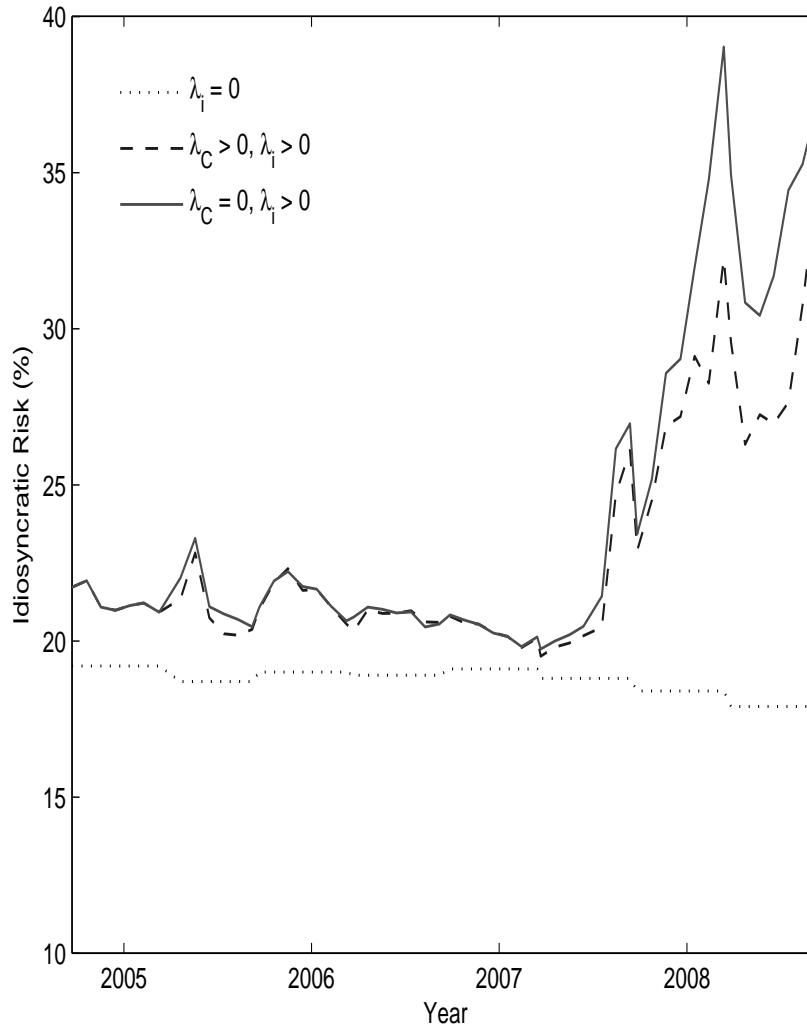


Figure IA.6. Total idiosyncratic risk. This figure presents the estimated total idiosyncratic risk ($\sqrt{\sigma_i^2 + y_i^2 \lambda_{i,1}^Q}$) across the different models. $\lambda_i = 0$ presents the time-series estimates of idiosyncratic asset volatility (as in Table II). $\lambda_C > 0, \lambda_i > 0$ presents the estimated total idiosyncratic risk of the model with catastrophic jump risk. $\lambda_C = 0, \lambda_i > 0$ presents the estimated total idiosyncratic risk of the model without catastrophic jump risk.